Citation for published version:
Yates, CA 2014, 'Discrete and continuous models for tissue growth and shrinkage', Journal of Theoretical Biology, vol. 350, pp. 37-48. https://doi.org/10.1016/j.jtbi.2014.01.041

DOI:
10.1016/j.jtbi.2014.01.041

Publication date:
2014

Document Version
Peer reviewed version

Link to publication

Publisher Rights
CC BY-NC-ND

The published version is available via: http://dx.doi.org/10.1016/j.jtbi.2014.01.041

University of Bath

General rights
Copyright and moral rights for the publications made accessible in the public portal are retained by the authors and/or other copyright owners and it is a condition of accessing publications that users recognise and abide by the legal requirements associated with these rights.

Take down policy
If you believe that this document breaches copyright please contact us providing details, and we will remove access to the work immediately and investigate your claim.

Download date: 13. May. 2019

Author's Accepted Manuscript

www.elsevier.com/locate/yjtbi

Discrete and continuous models for tissue growth and shrinkage

Christian A. Yates

PII: S0022-5193(14)00060-5
DOI: http://dx.doi.org/10.1016/j.jtbi.2014.01.041
Reference: YJTBI7595

To appear in: *Journal of Theoretical Biology*

Received date: 2 September 2013
Revised date: 14 January 2014
Accepted date: 31 January 2014

Cite this article as: Christian A. Yates, Discrete and continuous models for tissue growth and shrinkage, *Journal of Theoretical Biology*, http://dx.doi.org/10.1016/j.jtbi.2014.01.041

This is a PDF file of an unedited manuscript that has been accepted for publication. As a service to our customers we are providing this early version of the manuscript. The manuscript will undergo copyediting, typesetting, and review of the resulting galley proof before it is published in its final citable form. Please note that during the production process errors may be discovered which could affect the content, and all legal disclaimers that apply to the journal pertain.

ACCEPTED MANUSCRIPT

Discrete and continuous models for tissue growth and shrinkage

Christian A. Yates[a,*]

[a] *Mathematical Institute, Andrew Wiles Building, University of Oxford, Radcliffe Observatory Quarter, Woodstock Road, Oxford, OX2 6GG, United Kingdom*

Abstract

The incorporation of domain growth into stochastic models of biological processes is of increasing interest to mathematical modellers and biologists alike. In many situations, especially in developmental biology, the growth of the underlying tissue domain plays an important role in the redistribution of particles (be they cells or molecules) which may move and react atop the domain. Although such processes have largely been modelled using deterministic, continuum models there is an increasing appetite for individual-based stochastic models which can capture the fine detail of the biological movement processes which are being elucidated by modern experimental techniques, and also incorporate the inherent stochasticity of such systems.

In this work we study a simple stochastic model of domain growth. From a basic version of this model, Hywood et al. [J.D. Hywood, E.J. Hackett-Jones, and K.A. Landman. Modelling biological tissue growth: discrete to continuum representations. *Phys. Rev. E*, 88(3):032704, 2013] were able to derive a Fokker-Plank equation (FPE) (in this case an advection-diffusion partial differential equation on a growing domain) which describes the evolution of the probability density of some tracer particles on the domain. We extend their work so that a variety of different domain growth mechanisms can be incorporated and demonstrate a good agreement between the mean tracer density and the solution of the FPE in each case. In addition we incorporate domain shrinkage (via element death) into our individual-level model and demonstrate that we are able to derive coefficients for the FPE in this case as well. For situations in which the

*Corresponding author
Email address: yatesc@maths.ox.ac.uk (Christian A. Yates)
URL: http://people.maths.ox.ac.uk/yatesc/ (Christian A. Yates)

Accepted manuscript

ACCEPTED MANUSCRIPT

drift and diffusion coefficients are not readily available we introduce a numerical coefficient estimation approach and demonstrate the accuracy of this approach by comparing it with situations in which an analytical solution is obtainable.

1. Introduction

There are many biological scenarios in which tissue growth plays a significant role in the distribution of migrating cells. Embryogenesis is one such process which provides numerous demonstrations of the importance of domain growth to the final positions of various cell types. At the same time as the embryo is growing the organisation of complex biological superstructures (such as limbs) is being orchestrated [5], therefore it is vital that the processes of cell migration and domain growth are coordinated with each other in order to achieve the correct results [37]. For example, McLennan et al. [28] examined how a subpopulation of neural crest cells travelled long distances and responded to growth of the underlying tissue. They found, not only that cells are carried by the tissue growth, but also that cellular velocity profiles correspond to the logistic tissue growth.

There have been several theoretical studies of the interplay between domain growth and pattern formation in both deterministic [30, 10, 9, 11, 7, 22] and stochastic [38] regimes. Others investigations have specifically focussed on the targeted migration of cells on growing domains and have again covered both the deterministic [26, 32] and stochastic [4, 3] scenarios and indeed mechanisms in order to segue between the two [2, 40]. The two types of modelling regime traditionally focus on different scales, with stochastic models able to incorporate experimental scale details and the inherent noisiness of the biological system, while deterministic, continuum models tend to focus on the macroscale, ensemble properties and give a clear overview of the behaviour of the system. A multiscale understanding of the complex processes involved with cell migration can be achieved by linking these two modelling regimes together in an 'equivalence framework' which provides insight into the interplay between the individual-level and population-level models. Employing such an equivalence framework allows us to make use of either modelling regime in order to investigate the relevant properties of the system.

Accepted manuscript

ACCEPTED MANUSCRIPT

Recently Hywood et al. [18] have initiated such a framework by analysing a discrete, stochastic, on-lattice domain growth model in which the domain is made up of elements which may proliferate independently and with equal probability. Using the infinitesimal moments of the underlying stochastic process [14, 19] the authors were able to derive the coefficients of a Fokker-Planck equation (FPE) which approximates the spatio-temporal evolution of the expected occupancy of the lattice sites in the case of an exponentially growing domain. The work of Hywood et al. [18] is itself an extension of the work of Binder and Landman [3] who consider a similar process on a deterministically growing domain.

In Section 2 we review the work of Hywood et al. [18] and describe how it might be extended to include time-dependent proliferation rates and to incorporate elemental death. Using this reformulated model we are able to extend this equivalence framework, in Section 3, to cases where the domain does not grow exponentially in the mean-field. By deriving the infinitesimal moments of the stochastic process which underlies domain growth we are able to incorporate several biologically-motivated types of domain growth including exponential, linear and logistic. Importantly, in Section 4 we also consider the case in which individual elements are allowed to die as well as proliferate. We derive the drift and diffusion coefficients of the FPE which describes the expected marker density on the growing/contracting domain. Not only does this allow for the more realistic representation of domain growth processes in which apoptosis may occur, but it also enables the representation of domain shrinkage which may be important for biological processes such as wound healing [16, 17]. In each situation we confirm our theoretical findings by comparisons of the mean tracer density (over many realisations of the individual-level model) to numerical solutions of the derived FPEs.

There are situations in which the drift and diffusion coefficients of the underlying stochastic process are not readily available. In order to deal with these situations, in Section 5, we present a Fokker-Plank coefficient estimation approach [39] which is reminiscent of the equation-free technique [20]. We utilise this approach in order to find computationally the coefficients of the assumed FPE and we verify our findings through further numerical simulations.

Accepted manuscript

ACCEPTED MANUSCRIPT

We conclude in Section 6 with a brief discussion summarising our findings and suggesting areas into which this work may be extended.

2. An equivalence framework

In this section we introduce the individual-based model and the continuum representation between which we hope to derive an equivalence framework. We extend the basic individual-based model to incorporate time-dependent proliferation rates and elemental death and present the FPE which we expect to describe the mean-field tracer density.

2.1. The individual-based model

We begin by introducing the basic stochastic model upon which the rest of the results of this paper are based. Consider a one-dimensional domain of made up initially of N_0 contiguous elements each of length Δ. We incorporate growth and shrinkage into this individual-level model by allowing these elements to undergo 'proliferation events' and 'death events' which are analogous to biological cell division and cell death events[1]. In continuous time a domain element is chosen, uniformly amongst all the elements, to proliferate or to die with exponentially distributed waiting time. We extend the work of Hywood et al. [18] by introducing time-dependence of the parameter, $b(t)$, of the exponential waiting time distribution for birth events. This allows us to incorporate a variety of different types of domain growth in addition to the standard exponential domain growth resultant from a time-independent waiting time distribution. In addition we incorporate the possibility of a time-dependent rate of death, $d(t)$ into the model.

If domain element i is chosen to proliferate then it does so by pushing all the elements to its right (including itself) a distance Δ to the right in order to make room for an identical daughter element which is placed in its original position (see Fig 1). If element i is selected to die then it is removed from the lattice and all the elements to its right shift Δ to the left in order to fill the gap left by its removal (see Fig 2). In order to better understand the dynamics of the domain

[1] We note that biological cells do not instantaneously disappear, grow or divide, nor do they have exponentially distributed waiting times between divisions. These are, however, mathematical idealisations that we have made in order to render the model tractable.

Accepted manuscript

ACCEPTED MANUSCRIPT

growth/shrinkage process we can place tracer particles on top of a subset of the domain elements. We say that these domain elements are 'marked'. In general these tracer particles move with the domain elements with which they are initially associated. In order to complete the specification of the general individual-level model it is necessary to describe what happens to such tracer particles upon proliferation/death of the 'marked' element with which they are associated. In a proliferation event the tracer particle moves Δ to the right with the domain element which was selected to proliferate (see Fig 1 (b)). However, with a death event the tracer particle remains in the lattice site it currently occupies and becomes associated with the domain element which shifts to the left in order to occupy the vacant lattice site (see Fig. 2 (b) and (c)). There is no limit to the number of tracer particles that can be associated with a single lattice element. The aim of this paper is to derive a partial differential equation (PDE) which describes the average behaviour of these tracer particles.

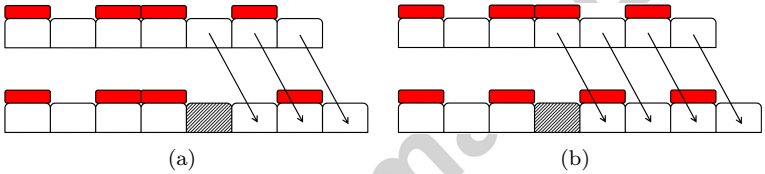

Figure 1: *Examples of growth and division events. Domain elements are white boxes and tracer particles are represented by smaller red boxes atop particular 'marked' elements. In each subfigure the top configuration shows a domain before a growth event and the bottom a domain configuration after a growth event. (a) An unmarked element is chosen to divide. It does so by pushing itself and the intervals to its right one element length, Δ. Tracer particles move with the elements and a new element (hatched) is inserted in the empty space. (b) A marked element is selected to divide. It undergoes the same movement procedure as for the unmarked element taking its tracer particle with it. Again a new element (hatched) is inserted in the vacant space.*

2.2. The Fokker-Planck equation

In particular we aim to derive the coefficients of an FPE which describes the average density of the tracer particles situated on the domain. If we define the random variable $M_i(t)$ to be the number of tracer particles associated with the element at lattice site i, then we can denote the expected occupancy of site i as

$$C_i(t) = \mathbb{E}[M_i(t)]. \tag{1}$$

ACCEPTED MANUSCRIPT

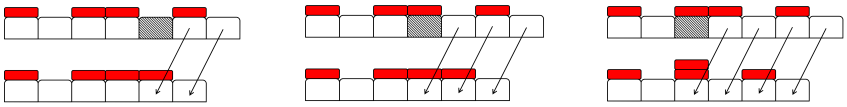

Figure 2: *Examples of element death events. Domain elements are white boxes and tracer particles are represented by smaller red boxes atop particular 'marked' elements. In each subfigure the top configuration shows a domain before a death event and the bottom a domain configuration after a death event. (a) An unmarked element (hatched) is chosen to die. It is removed from the domain and intervals to its right move leftwards by one element length, Δ, to fill the space. Tracer particles move with their elements. (b) A marked element (hatched) is chosen to die. It is removed from the domain. However its tracer particle remains in place. The elements to the right of the dead element move to the left one element length, Δ, and a previously unmarked element becomes marked. (c) A marked element (hatched) dies and is removed. Its tracer particle remains where it is and causes the already marked element that was immediately to the right of the dead element to become doubly marked as it moves into the vacant space. There is no limit to how many tracer particles an element can accrue.*

We can then derive a Fokker-Planck equation for the evolution of $C(x,t)$, the continuous-space function approximating the expected density variables $C_i(t)$, using the infinitesimal moments [14, 19] of the random variable $X(t)$ which denotes the position, at time t, of an element initially at $X(0) = X_0$, as in Hywood et al. [18]. Specifically we use the infinitesimal mean

$$\mu(x,t) = \lim_{h\to 0} \frac{1}{h}\mathbb{E}[X(t+h) - X(t)|X(t) = x], \tag{2}$$

and the infinitesimal variance

$$\sigma^2(x,t) = \lim_{h\to 0} \frac{1}{h}\mathrm{var}(X(t+h) - X(t)|X(t) = x), \tag{3}$$

which are the drift and diffusion coefficients in the associated Fokker-Planck equation [14, 19]:

$$\frac{\partial C}{\partial t} = -\frac{\partial}{\partial x}[\mu(x,t)C(x,t)] + \frac{\partial^2}{\partial x^2}\left[\frac{1}{2}\sigma^2(x,t)C(x,t)\right]. \tag{4}$$

Note that, in contrast to the case of the time-independent birth rate, our infinitesimal moments will depend explicitly on time. Our task now, for a wide range of different random variables, $X(t)$, resultant from a variety of time-dependent waiting time distributions, is to determine the first two infinitesimal moments in order to populate the resultant Fokker-Planck equation (4).

Accepted manuscript

ACCEPTED MANUSCRIPT

3. Infinitesimal moments for time-dependent growth rates

By allowing the rate of element addition, $b(t)$, to depend on time we are able to incorporate a wide range of different types of domain growth into the individual-based model. Since each element proliferates independently of the other elements we may write down a probability master equation for the number of elements, $K(t)$, populating the domain at time, t:

$$\frac{\mathrm{d}P(K=k,t)}{\mathrm{d}t} = b(t)\left((k-1)P(K=k-1,t) - kP(K=k,t)\right), \tag{5}$$

with initial condition

$$P(K=k,0) = \begin{cases} 1, & \text{if } K=K_0, \\ 0, & \text{otherwise.} \end{cases} \tag{6}$$

From equation (5) we can derive an equation for the mean number of elements, $K_m(t)$, which populate the domain at time t:

$$\frac{\mathrm{d}K_m}{\mathrm{d}t} = b(t)K_m, \tag{7}$$

with initial condition $K_m(0) = K_0$. Therefore, the mean length of the domain, $L = \Delta K_m$, satisfies

$$\frac{\mathrm{d}L}{\mathrm{d}t} = b(t)L, \tag{8}$$

with initial condition $L(0) = L_0 = \Delta K_0$. Using this equation we can directly link the choice of $b(t)$ to the resulting expected time-dependent length of the domain, $L(t)$.

Given $b(t)$ we can also derive the infinitesimal moments of a general time-dependent birth process, which will allow us to define the continuous-space Fokker-Planck equation associated with the individual-level model, as follows.

We begin by deriving the continuous-time master equation for a time-dependent integer-valued birth process, $Y(t) = X(t)/\Delta$ which describes the probability, $p(Y(t+h) = N|Y(t) = n_0)$ of a domain element at position $x = n_0\Delta$ at time t being found at position $x = N\Delta$ at time $t+h$, which we will denote as $p_N^t(h)$. In order to derive a master equation for this process we consider a small time interval δh in which the probability of more than one birth event is $o(\delta h)$ so

Accepted manuscript

ACCEPTED MANUSCRIPT

that we may write

$$p_N^t(h+\delta h) = (1-b(t+h)N\delta h)p_N^t(h) + b(t+h)(N-1)p_{N-1}^t(h)\delta h + o(\delta h). \quad (9)$$

Since we are considering a continuous time Markov process we may rearrange equation (9) as

$$\frac{\mathrm{d}p_N^t(h)}{\mathrm{d}h} = (N-1)b(t+h)p_{N-1}^t(h) - Nb(t+h)p_N^t(h), \quad (10)$$

with initial condition

$$p_N^t(0) = \begin{cases} 1, & \text{if } N = n_0, \\ 0, & \text{otherwise.} \end{cases} \quad (11)$$

In order to solve recurrence relation (10) for $p_N^t(h)$ we consider the probability generating function, $G(z,h) = \mathbb{E}(z^X) = \sum_{N=n_0}^{\infty} z^N p_N^t(h)$. Then equation (10) becomes a first order linear PDE

$$\frac{\partial G}{\partial h} = z(z-1)(b(t+h))\frac{\partial G}{\partial z}, \quad (12)$$

with initial condition

$$G(z,0) = z^{n_0}, \quad (13)$$

which we can solve using the method of characteristics [36] as

$$G(z,h) = \left[1 + \frac{1}{\frac{\exp(\rho(h))}{(z-1)} + (\exp(\rho(h)) - 1)}\right]^{n_0}, \quad (14)$$

where $\rho(h) = -\int_0^h b(t+\bar{h})\mathrm{d}\bar{h}$. From here we can expand $G(z,h)$ in powers of z in order to find that $p_N^t(h)$ follows a negative binomial distribution

$$p_N^t(h) = \binom{N-1}{n_0-1}(1-\exp(\rho(h)))^{N-n_0}(\exp(\rho(h)))^{n_0}, \quad (15)$$

and use this to calculate the moments. Alternatively, we can recognise (using the properties of probability generating functions) that the first and second moments are given by

$$\mathbb{E}[Y(t+h)] = \lim_{z\uparrow 1} G'(z,h) = n_0 e^{-\rho(h)}. \quad (16)$$

Accepted manuscript

ACCEPTED MANUSCRIPT

and

$$\begin{aligned}\text{var}[Y(t+h)] &= \lim_{z\uparrow 1}\left\{G''(z,h)+G'(z,h)-(G(z,h))^2\right\}\\ &= n_0e^{-\rho(h)}\left(1-e^{-\rho(h)}+2e^{-\rho(h)}\left(1-e^{\rho(h)}\right)\right) \qquad (17)\\ &= n_0e^{-\rho(h)}\left(e^{-\rho(h)}-1\right), \qquad (18)\end{aligned}$$

respectively, (where $'$ notes differentiation of $G(z,h)$ with respect to z). The infinitesimal moments for position, $X(t)$, can therefore be calculated as:

$$\begin{aligned}\mu(x,t) &= \lim_{h\to 0}\frac{1}{h}\left\{\mathbb{E}[X(t+h)|X(t)=x]-\mathbb{E}[X(t)|X(t)=x]\right\}\\ &= \Delta\lim_{h\to 0}\frac{1}{h}\left\{\mathbb{E}[Y(t+h)|Y(t)=x/\Delta]-\mathbb{E}[Y(t)|Y(t)=x/\Delta]\right\}\\ &= \Delta n_0\lim_{h\to 0}\frac{1}{h}(e^{-\rho(h)}-1), \qquad (19)\end{aligned}$$

and

$$\begin{aligned}\sigma^2(x,t) &= \lim_{h\to 0}\frac{1}{h}\left\{\text{var}(X(t+h)|X(t)=x)-\text{var}(X(t)|X(t)=x)\right\}\\ &= \Delta^2\lim_{h\to 0}\frac{1}{h}\text{var}(Y(t+h)|Y(t)=x/\Delta)\\ &= \Delta^2n_0\lim_{h\to 0}\frac{1}{h}e^{-\rho(h)}\left(e^{-\rho(h)}-1\right). \qquad (20)\end{aligned}$$

We can now use equations (19) and (20) to calculate the infinitesimal moments for a range of time-dependent element division rates.

3.1. Exponential domain growth

The elongation of the developing intestinal tract of the quail embryo can be well approximated by exponential growth [4] as can the growth of sections of the embryos of the alligator *Alligator mississippiensis* [29, 12]. Kulesa et al. [22] have studied the initiation and positioning of teeth primordia in the same alligator species. Using a reaction diffusion model they demonstrated that exponential jaw growth plays a crucial role in the developmental patterning of the tooth initiation process in agreement with corresponding experimental studies [33, 34, 35]. Exponential growth has also been found to model the early stages of unconstrained cancerous tumour growth Gerlee [13]. In addition, exponentially growing domains are a popular choice for mathematical studies of domain growth because of their straightforward implementation in both individual-based [2, 40, 3] and population-level models [26, 10, 9].

Accepted manuscript

ACCEPTED MANUSCRIPT

For simple exponential domain growth we choose the time-independent growth rate, $b(t) = b$. This choice determines $\rho(h) = -bh$ and consequently the infinitesimal moments as

$$\mu(x,t) = xb, \tag{21}$$

and

$$\sigma^2(x,t) = \Delta x b. \tag{22}$$

It is of comfort to note that our generalised formula gives the same infinitesimal moments as those derived by Hywood et al. [18] with the resulting PDE:

$$\frac{\partial C}{\partial t} = -b\frac{\partial}{\partial x}[xC(x,t)] + \Delta b \frac{\partial^2}{\partial x^2}\left[x\frac{1}{2}C(x,t)\right] \quad \text{for} \quad 0 < x < L(t), \tag{23}$$

where $L(t) = L_0 \exp(bt)$ is the mean domain length as defined by equation (8).

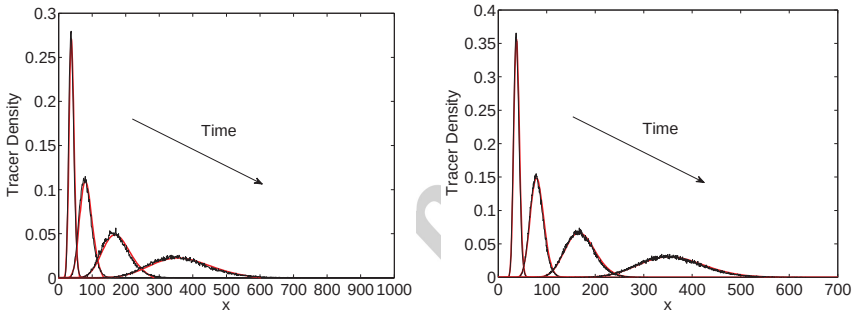

Figure 3: *A comparison of the expected occupancy of tracer particles on an exponentially growing domain in the stochastic and deterministic regimes at different times. The red curves represent the solution of the Fokker-Planck equation* (23) *and the (noisy) black curve represents the expected density of tracer particles averaged over 10,000 realisations of the individual based model. In both cases* $L(0) = 30$*, with tracer particles initially between* $15 \leq x \leq 20$*. The rate of element proliferation is* $b = 0.05$ *and the curves are plotted at* $t = 15, 30, 45, 60$*. (a)* $\Delta = 1$*, (b)* $\Delta = 1/2$*.*

Fig. 3 gives a comparison between the individual-level model and the PDE for two different values of Δ. The individual-level occupancy is averaged over 10,000 repeats of the stochastic simulation and the PDE is solved as described in the appendix. The agreement between the two regimes is excellent in both cases, but improves with decreasing Δ.

ACCEPTED MANUSCRIPT

3.2. Linear domain growth

The uniform exponential growth described above may be used to model a population of cells undergoing proliferation at a fixed rate, independent of space and time. While this might be a reasonable model of the initial stages of an unconfined growth it is not realistic for large times and is a poor model for domain growth in many application areas. In order to increase the biological applicability of the model we must consider more complex growth rates which conform to forms of macroscopic growth which are more relevant biologically. Linear growth, for example, is exhibited in the early development of some fish [21] and seeds [6]. It has also been found to model the growth of the body section of some alligator embryos [29]. In addition, linear growth has previously been investigated in deterministic mathematical models of cell migration and domain colonisation [26, 9].

Choosing $b(t) = r/(1 + rt)$ can be shown, using equation (8), to give linear domain growth of the form

$$L(t) = L_0(1 + rt), \tag{24}$$

in the mean field. Using equations (19) and (20) the corresponding infinitesimal moments are

$$\mu(x, t) = \frac{xr}{1 + rt}, \tag{25}$$

and

$$\sigma^2(x, t) = \frac{\Delta xr}{1 + rt}. \tag{26}$$

Fig. 4 gives a comparison between the individual-level model and the PDE for linear domain growth. The individual-level occupancy is averaged over 10,000 repeats of the stochastic simulation and the PDE is solved as described in the appendix. The agreement between the two regimes is good when $\Delta = 1$ (see Fig 4 (a)) and excellent when $\Delta = 1/2$ (see Fig 4 (b)). In particular, for $\Delta = 1$ we see that the FPE underestimates the density of tracer particles at the right-hand end of the domain where the infinitesimal moments are largest. This underestimation disappears as Δ decreases and the contributions of the higher order moments, which will be proportional to higher powers of Δ and are not

Accepted manuscript

ACCEPTED MANUSCRIPT

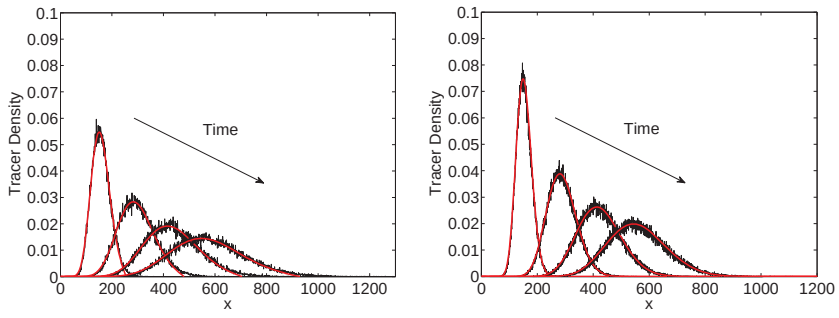

Figure 4: *A comparison of the expected occupancy of tracer particles on a linearly growing domain in the stochastic and deterministic regimes at different times. Figure descriptions and initial conditions are as in Fig. 3. The rate of element proliferation is given by* $b(t) = r/(1+rt)$ *with* $r = 0.5$ *and the curves are plotted at* $t = 15, 30, 45, 60$. *(a)* $\Delta = 1$, *(b)* $\Delta = 1/2$.

captured in the Fokker-Planck approximation, dissipate.

3.3. Logistic domain growth

McLennan et al. [28] found that the distance from the dorsal neural tube midline to the distal tip of the lateral mesoderm (a relevant cell migratory pathway) lengthens non-linearly, according to a logistic function, during cranial neural crest cell migration in chick embryos. In experiments on turtle and albatross embryos ([27] and [31] respectively) it has been shown that the mass of the embryo grows according to a logistic curve. It has also been postulated that logistic growth is a good model for the underlying tissue growth in cell migration models in several mathematical papers [26, 9].

Choosing

$$b(t) = \frac{r(\xi - 1)}{\xi + \exp(rt) - 1}, \tag{27}$$

and solving equation (8) for the mean domain length gives

$$L = \frac{L_0 \xi \exp(rt)}{\xi + \exp(rt) - 1}. \tag{28}$$

Substituting this back into equation (8) gives the recognisable differential equation for logistic growth

$$\frac{\mathrm{d}L}{\mathrm{d}t} = rL\left(1 - \frac{L}{L_0\xi}\right), \tag{29}$$

Accepted manuscript

ACCEPTED MANUSCRIPT

where ξ is the ratio between final and initial domain sizes[2] and r represents the growth rate. As before we can derive the infinitesimal moments using equations (19) and (20) as

$$\mu(x,t) = \frac{xr(\xi-1)}{\xi + \exp(rt) - 1}, \tag{30}$$

and

$$\sigma^2(x,t) = \frac{\Delta xr(\xi-1)}{\xi + \exp(rt) - 1}. \tag{31}$$

Numerical comparisons between the individual-level simulations and the PDE show good agreement with the same characteristic increase in accuracy with decreasing Δ (data not shown).

3.4. Gompertzian domain growth

Gompertzian growth, originally devised to model human mortality [15], has been used to model a wide range of biological growth, from organisms [24] through to organs [25] and the growth of cancerous tumours [23, 13]. In a one-dimensional context it has also been used to model the increase in the numbers of teeth of the alligator *Alligator mississippiensis* [22].

The differential equation for Gompertzian domain growth takes the form

$$\frac{\mathrm{d}L}{\mathrm{d}t} = rL\left(\ln\left(\frac{R}{L}\right)\right), \tag{32}$$

where r specifies the rate of growth and R represents the carrying capacity (i.e. the maximum length to which the domain can grow). This mean-field growth equation can be recapitulated by choosing

$$b(t) = r\ln\left(\frac{R}{L_0}\right)\exp(-rt). \tag{33}$$

Such a growth rate gives infinitesimal moments

$$\mu(x,t) = xr\exp(-rt)\ln\left(\frac{R}{L_0}\right), \tag{34}$$

[2] $L_0\xi$ is commonly denoted R, the maximum length to which the domain can grow or 'carrying capacity'.

Accepted manuscript

ACCEPTED MANUSCRIPT

and

$$\sigma^2(x,t) = \Delta x r \exp(-rt) \ln\left(\frac{R}{L_0}\right). \tag{35}$$

As with previous time-dependent domain growth mechanisms, numerical comparisons between the individual-level simulations and the PDE show good agreement, with increasing accuracy for decreasing Δ (data not shown).

3.5. Generalised logistic domain growth

We motivate the consideration of generalised logistic domain growth by highlighting that it incorporates both logistic and Gompertzian domain growth (see sections 3.3 and 3.4 respectively) as special cases. The additional parameter, ν, which allows us to move between these two important types of growth also allows us to capture many other types of biologically-relevant sigmoidal growth in between.

The differential equation which specifies generalised logistic growth is given by

$$\frac{\mathrm{d}L}{\mathrm{d}t} = rL\left(1 - \left(\frac{L}{R}\right)^{\nu}\right), \tag{36}$$

where r is the underlying rate of growth, R is the carrying capacity and ν is a tunable parameter which allows us to segue between different types of growth. In the limit $\nu \to 1$ we recapitulate equation (29) for logistic growth, whereas in the limit $\nu \to 0$ (and $r \propto 1/\nu$) we recapture the Gompertzian growth equation (32). A time-dependent birth rate which gives a mean domain length corresponding to generalised logistic domain growth is

$$b(t) = \frac{rQ\exp(-r\nu t)}{1 + Q\exp(-r\nu t)}, \tag{37}$$

where

$$Q = \left(\frac{R}{L_0}\right)^{\nu} - 1. \tag{38}$$

Predicated on this birth rate, the required infinitesimal moments are

$$\mu(x,t) = \frac{xrQ}{\exp(r\nu t) + Q}, \tag{39}$$

and

$$\sigma^2(x,t) = \frac{\Delta x r Q}{\exp(r\nu t) + Q}. \tag{40}$$

Accepted manuscript

ACCEPTED MANUSCRIPT

It is of comfort to note that the limits $\nu \to 1$ and $\nu \to 0$ (and $r \propto 1/\nu$) return us to the infinitesimal moments derived for the logistic and Gompertzian growth regimes respectively.

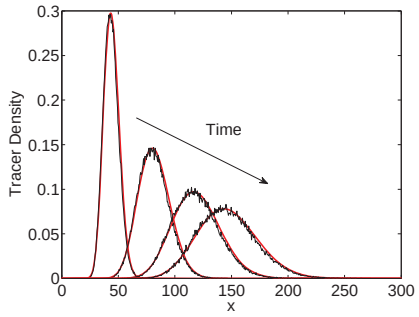

Figure 5: *A comparison of the expected occupancy of tracer particles on a domain growing according to generalised logistic growth in the stochastic and deterministic regimes at different times with* $\Delta = 1/2$. *Figure descriptions and initial conditions are as in Fig. 3. The rate of element proliferation is given by equation* (37) *with* $r = 0.1$, $R = 300$ *and* $\nu = 0.5$. *The curves are plotted at* $t = 15, 30, 45, 60$.

Fig. 5 demonstrates a comparison between the expected tracer densities of the two modelling regimes for generalised logistic domain growth. The agreement is good. As before, for larger values of Δ, the absence of the contribution of the higher order moments of the process to the FPE description mean that the PDE underestimates the individual-level density at the right hand side of the domain, where those moments are largest.

4. Incorporating element death

Although the representation of domain growth is clearly important for the modelling of many areas of development [29, 4, 30, 28, 27, 31] the representation of domain shrinkage also has relevant application areas including wound healing [16, 17], for example. The incorporation of element death is important in situations where domain elements may proliferate and die even if the net growth rate is positive: it might be argued that domain growth in which element death is possible but the growth rate, $b(t)$, outweighs the death rate, $d(t)$, can be modelled using a purely growing domain with a reduced positive growth rate, $\lambda(t) = b(t) - d(t)$. However, this argument is incorrect since, although the mean growth rate may be estimated correctly, the second and higher order moments of the process will be incorrect. In particular, one stark difference is

Accepted manuscript

ACCEPTED MANUSCRIPT

that the domain in which death is incorporated explicitly will shrink to zero size with a non-zero probability, whereas there is no possibility of this happening in the purely growing domain with reduced net growth rate. In this section we incorporate elemental death into the model of domain growth and also consider a pure domain shrinkage model.

4.1. Mixed birth and death

If we continue to include elemental proliferation at a rate $b(t)$, but also introduce elemental death at a rate $d(t)$ then the equation describing the mean domain length becomes

$$\frac{\mathrm{d}L}{\mathrm{d}t} = (b(t) - d(t))L, \tag{41}$$

as one might reasonably expect considering the derivation of equation (8). The initial condition is, as before, $L(0) = L_0 = \Delta K_0$, where K_0 is the initial number of elements populating the domain and Δ the length of each of those elements.

In addition the probability master equation which describes the probability, $p_N^t(h)$, of a domain element at position $x = n_0\Delta$ at time t being found at position $x = N\Delta$ at time $t + h$ is given by

$$\frac{\mathrm{d}p_N^t(h)}{\mathrm{d}h} = (N-1)b(t+h)p_{N-1}^t(h)+(N+1)d(t+h)p_{N+1}^t(h)-N(b(t+h)+d(t+h))p_N^t(h), \tag{42}$$

with the same initial condition as in the pure birth process, given by equation (11). Note now that N is not necessarily greater than n_0 as it was in the pure birth process. Appealing again to the probability generating function, $G(z, t)$, we can reduce equation (42) to a first order linear PDE

$$\frac{\partial G}{\partial h} = (z-1)(b(t+h)z - d(t+h))\frac{\partial G}{\partial z}, \tag{43}$$

with initial condition

$$G(z, 0) = z^{n_0}. \tag{44}$$

This PDE can be solved using the method of characteristics [36] to give

$$G(z,h) = \left[1 + \frac{1}{\frac{\exp(\rho(h))}{(z-1)} - \int_0^h b(t+\bar{h})\exp(\rho(\bar{h}))\mathrm{d}\bar{h}}\right]^{n_0}, \tag{45}$$

Accepted manuscript

ACCEPTED MANUSCRIPT

where now $\rho(h) = \int_0^h d(t+\bar{h}) - b(t+\bar{h})\mathrm{d}\bar{h}$.

We can expand $G(z,h)$ in powers of z in order to find the explicit probability distribution $p_N^t(h)$:

$$p_N^t(h) = \sum_{j=0}^{\min(n_0,N)} \binom{n_0}{j} \binom{N+n_0-j-1}{n_0-1} \alpha^{n_0-j}\beta^{N-j}(1-\alpha-\beta)^j, \qquad (46)$$

where

$$\alpha = 1 - \frac{1}{\chi(h)}, \qquad (47)$$

and

$$\beta = 1 - \frac{\exp(\rho(h))}{\chi(h)}, \qquad (48)$$

with

$$\chi(h) = \exp(\rho(h)) + \int_0^h b(t+\bar{h})\exp(\rho(\bar{h}))\mathrm{d}\bar{h}, \qquad (49)$$

and use this to calculate the moments. Alternatively (and more straightforwardly), we can use the properties of probability generating functions in order to find the infinitesimal moments as

$$\mu(x,t) = \Delta n_0 \lim_{h\to 0} \frac{1}{h}\left(e^{-\rho(h)} - 1\right), \qquad (50)$$

and

$$\sigma^2(x,t) = \Delta^2 n_0 \lim_{h\to 0} \frac{1}{h} e^{-\rho(h)}\left(1 - e^{-\rho(h)} + 2e^{-\rho(h)}\int_0^h b(t+\bar{h})e^{\rho(\bar{h})}\mathrm{d}\bar{h}\right), \qquad (51)$$

respectively.

For simplicity we let the birth and death rates b and d take constant values in what follows, although we stress that the infinitesimal moments we have derived (see equations (50) and (51)) are for general time-dependent birth and death rates.

We emphasise the importance of explicitly considering elemental death as well as birth: consider a domain which is initially populated with n_0 domain elements. Then we can use equation (46) to calculate the probability that all the elements of the domain die, $p_0(\infty)$ (i.e. that the domain size reduces to zero). We find that

$$p_0(\infty) = \begin{cases} 1 & \text{if } b \le d, \\ \left(\frac{d}{b}\right)^{n_0} & \text{if } b > d. \end{cases} \qquad (52)$$

Accepted manuscript

ACCEPTED MANUSCRIPT

When the rate of element death outweighs that of element proliferation the domain is certain to shrink to zero as time progresses. However, even when the rate of element proliferation is greater than the rate of element death there is still a non-zero probability of domain extinction. Although, in a biological context, we may not be interested in the long-time behaviour of the domain, this extreme example serves to illustrate the point that simply considering the net rate of growth may not be sufficient to capture the detailed domain expansion behaviour.

The importance of considering elemental death as well as division is re-enforced by calculating the infinitesimal moments of the stochastic process. We use equations (50) and (51) to find

$$\mu(x,t) = x(b-d), \tag{53}$$

and

$$\sigma^2(x,t) = \Delta x(b+d). \tag{54}$$

If we choose the net growth rate $b-d$ to match that given in the pure exponential birth process of Section 3.1 then the advective terms in the Fokker-Planck equations corresponding to the infinitesimal means will match, however, the diffusive terms corresponding to the infinitesimal variances will differ.

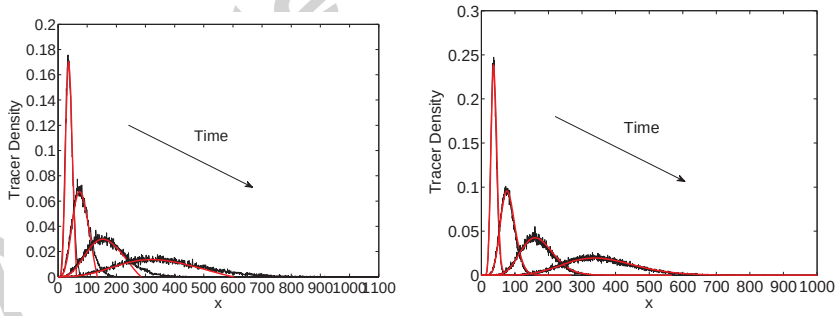

(a) (b)

Figure 6: *A comparison of the expected occupancy of tracer particles on a domain growing with constant birth and death rates, $b > d$ in the stochastic and deterministic regimes at different times with. Figure descriptions and initial conditions are as in Fig. 3. The rate of element proliferation is $b = 0.1$ and the rate of element death is $d = 0.05$, giving net growth rate $b - d = 0.05$ as in Fig. 3. The curves are plotted at $t = 15, 30, 45, 60$. (a) $\Delta = 1$, (b).*

ACCEPTED MANUSCRIPT

Fig. 6 demonstrates the importance of considering elemental death as well as growth. The net growth rate is $\lambda = b - d = 0.05$, the same as that given in Fig. 3, but because we are considering both birth and death the behaviour of both the PDE and the individual-based model are markedly different from those of the pure growth model. By time $t = 60$ it is clear to see that the tracer particles in this mixed birth and death process have spread much further than in the pure growth process of Section 3.1, (note the different scales on the x-axes of the two figures.). The underestimation of the tracer density at the right hand end of the domain for large values of Δ (see Fig. 6 (a)) is also much more pronounced in this mixed birth and death regime. This is because higher order moments neglected in the PDE description are larger and so the disparity between the two modelling regimes is greater. However, even with Δ as large as 1/2 (see Fig. 6 (b)) we see an excellent agreement between the two models.

4.2. Domain shrinkage

For completeness we include an example of domain shrinkage through a pure death process. The constant rate of elemental death is given by $d = 0.05$. The first two infinitesimal moments can be calculated as

$$\mu(x,t) = -xd, \tag{55}$$

and

$$\sigma^2(x,t) = \Delta x d. \tag{56}$$

For reasons discussed previously, in Fig. 7 (a), for long times we see that there is a significant disparity between the FPE solution and the individual-based simulations at the right-hand end of the domain for large Δ. Generally though, the agreement between the FPE solution and the mean tracer density in the individual-based model is excellent.

It is interesting to note that the support of the profile reduces with time and the height of the peak increases giving the simulations the look of a reaction/advection-diffusion equation running in reverse. If the time arrow on the figures were to be removed it would be easy to assume that the density profile evolves from left to right instead of the other way around. Since the backwards diffusion equation is known to be unstable this cannot be what is happening here, since our solution

Accepted manuscript

ACCEPTED MANUSCRIPT

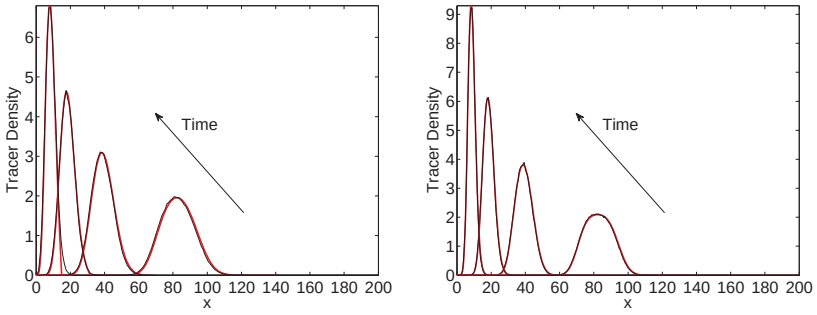

(a) (b)

Figure 7: *A comparison of the expected occupancy of tracer particles on a domain growing with constant death rate, d in the stochastic and deterministic regimes at different times. Figure descriptions are as in Fig. 3. In both cases $L(0) = 300$, with tracer particles initially between $150 \leq x \leq 200$. The rate of element death is $d = 0.05$. The curves are plotted at $t = 15, 30, 45, 60$. Note that the time arrow is in the opposite direction to previous figures, since the domain shrinks as time progresses. (a) $\Delta = 1$, (b) $\Delta = 1/2$.*

is stable. In order to gain a greater insight into what is actually happening we can expand the governing FPE:

$$\frac{\partial C}{\partial t} = dC(x,t) + d\left(x + \frac{\Delta}{2}\right)\frac{\partial C(x,t)}{\partial x} + \frac{dx\Delta}{2}\frac{\partial^2 C(x,t)}{\partial x^2}. \tag{57}$$

The diffusivity is, of course, positive since it is proportional to the infinitesimal variance, $\sigma^2(x,t)$. There is an advection term in the negative x-direction which is larger for larger values of x, causing the profile to shrink. In addition there is a source term which is proportional to $C(x,t)$ which is responsible for the appearance of the exponentially decaying tails of the profile.

5. Fokker-Plank coefficient estimation approach

For some growth rates specified in the individual-level model it may not be possible to derive analytically the coefficients of the FPE which corresponds to the tracer density. In such situations we require an alternative method in order to derive the FPE coefficients. In this section we introduce a method which allows us to approximate numerically the coefficients of such an FPE. Our method is reminiscent of the equation-free method [20], a computer-aided multiscale methodology which enables models at a fine/microscopic level to inform models at a coarse/macroscopic level through a series of *appropriately initialised* realisations of the microscopic model. Traditionally the equation-free

Accepted manuscript

ACCEPTED MANUSCRIPT

technique has been used to coarse-grain microscopic models when the macroscopic evolution equations exist conceptually, but are not available in a simple closed form. This is analogous to the situation we face when attempting to derive the coefficients of an FPE corresponding to the individual-level growth model for which the functional form of the growth rate precludes the use of analytical methods for deriving the FPE coefficients.

Our computer-assisted approach will allow us to determine the dependency of the drift and diffusion coefficients on the time and space variables. Specifically, given a simulation in a particular configuration at time, t, we can run the microscopic model forward a short period of time, δt, in order to determine where each tracer particle resides at time $t + \delta t$. If we repeat this sufficiently many times we may approximate the mean and standard deviation of the displacement of each tracer particle at a given time and space. The appropriate approximations for the drift and diffusion coefficients are therefore given by

$$\mu_{\delta t}(x,t) = \frac{1}{\delta t}\left\langle X(t+\delta t) - X(t) | X(t) = x \right\rangle, \tag{58}$$

$$\sigma^2_{\delta t}(x,t) = \frac{1}{\delta t}\left\{ \left\langle (X(t+\delta t) - X(t))^2 | X(t) = x \right\rangle - \mu_{\delta t}(x,t)^2 \right\}, \tag{59}$$

respectively, where $\langle \cdot \rangle$ denotes the average over many appropriately initialised simulations.

We note that these approximations to the drift and diffusion coefficient become exact (see equations (2) and (3)) in the limit $\delta t \to 0$. In a computational simulation, however, we cannot realise this limit. Instead continuous time is divided into a discrete mesh of spacing δt. For each point of this time mesh we approximate the drift and diffusion coefficients for each of the spatial lattice sites naturally defined by the individual-level simulation. It may appear that the smaller the value of δt the more accurate an approximation we will achieve to the drift and diffusion coefficients. Whilst in theory this is true, since only a finite number of realisations of the microscopic system are possible, taking a value of δt which is too small will result in regions of the time mesh for which we have few or no data points over which to average. This will lead to noisy or absent data points in our approximations. In practice there is a balance to be struck between taking δt small enough so as to achieve an accurate approximation at a fine resolution, and taking δt large enough to ensure each x and t

Accepted manuscript

ACCEPTED MANUSCRIPT

pair have sufficient data points in order to that we may calculate a meaningful average.

In order to ensure that the short bursts of simulation of the microscopic model are appropriately initialised, we simply run several repeats of the individual-based model recording the positions and times of each proliferation/death event. For each point in the time mesh we can extract the positions of each of the elements populating the domain at the current time point and subsequently calculate their positions at the next time point. Using these quantities it is straightforward to approximate the drift and diffusion coefficients of the microscopic process as in equations (58) and (59).

As an example we have approximated the drift and diffusion coefficients of the exponential domain growth process (see Fig. 8). These should be compared to the analytical formulae (21) and (22) respectively.

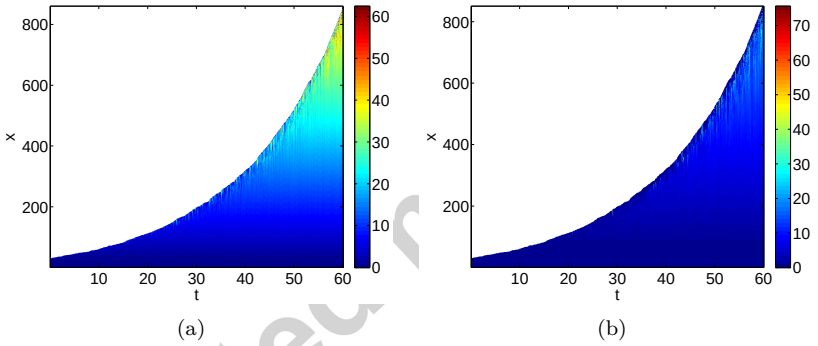

Figure 8: *The approximated (a) drift, $\mu_{\delta t}(x,t)$, and (b) diffusion, $\sigma^2_{\delta t}(x,t)$, coefficients. The linear dependence on x and the independence of t appear in both coefficients. The colour bars in both subfigures are distorted by the randomness in the approximations of the coefficients for large x (for a given time) where only a few instances of that length at that time have been realised, making the approximation noisier than at other points in the domain. Parameters are as in Fig. 3 with $\Delta = 1/2$ and time-interval $\delta t = 0.1$. The approximations are made by averaging over 1000 realisations of the individual-level model.*

Since, in this paper, we are considering uniform (isotropic) domain growth we can determine *a priori* that the drift coefficient will depend linearly on the spatial variable. In addition, in the case of purely time-dependent birth and death rates the diffusion coefficient will also depend linearly on the spatial variable. In order to demonstrate this principle we have averaged the approximated drift and diffusion coefficients of the exponential domain growth process over the

ACCEPTED MANUSCRIPT

realisations of the temporal mesh in order to show their linear dependence on x (see Fig. 9 (a)). As a result of this linear dependence it is possible to average over all the realisations in the spatial mesh and, adjusting for the position of the elements, calculate a more accurate approximation for the time-dependence of the drift and diffusion coefficients. We give a demonstration of the temporal dependence of the drift and diffusion coefficients for the uniform exponential domain growth process in Fig. 9 (b). The agreement with the result derived analytically is good for both coefficients.

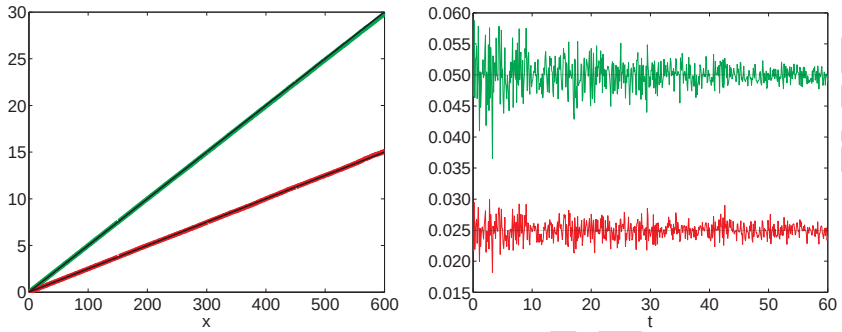

(a) (b)

Figure 9: *The dependence of the approximated drift (green) and diffusion (red) coefficients on (a) x (b) t. The analytically derived values are plotted in black for comparison. The approximation to the temporal dependence is noisier for small times where the average time-step of the individual-based model is large and fewer proliferation events occur per fixed time-step, δt. Parameters are as in Fig. 8.*

We note that, although the drift coefficient will always depend linearly on the spatial variable in a uniform (isotropic) domain growth process, in general the diffusion coefficient will not. The coefficient estimation approach will still be applicable, however the diffusion coefficient will need to be approximated explicitly for every space and time point (as in Fig. 8) rather than being averaged over the space coordinate. Similarly the coefficient estimation approach will still be applicable for non-uniform (anisotropic) domain growth processes, but both the drift and diffusion coefficients will need to be approximated explicitly for every space and time point.

Fig. 10 displays two further confirmatory examples of the agreement between time-dependence of the analytically derived and approximated drift and diffusion coefficients for two other ((a) linear and (b) Gompertzian) time-dependent processes. The agreement is excellent in both cases. The PDE solutions found

ACCEPTED MANUSCRIPT

using these drift and diffusion coefficients[3] are compared to the individual level simulations for linear and Gompertzian domain growth in Fig. 11 (a) and (b) respectively. We find that the agreement is good in both cases, although not as good as in the situation in which we employed the analytical expression for the drift and diffusion coefficients in order to solve the PDE.

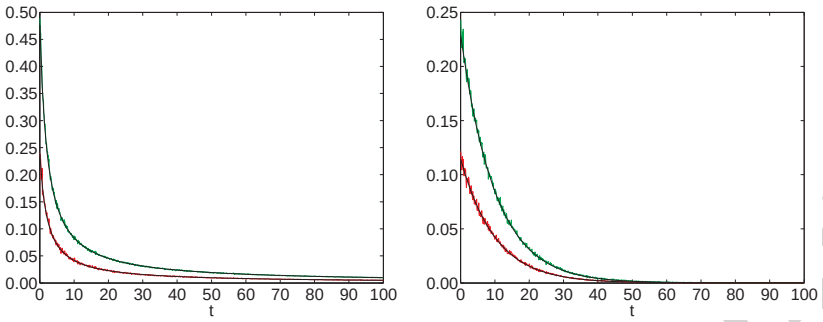

(a) (b)

Figure 10: *The dependence of the approximated drift (green) and diffusion (red) coefficients on t for (a) linear domain growth and (b) Gompertzian domain growth. The analytically derived values are plotted in black for comparison. Parameters for (a) are as in Fig. 4. Parameters for (b) are* $L_0 = 30$, $r = 0.1$ *and* $R = 300$. *In both cases* $\Delta = 1/2$, $\delta t = 0.1$ *and coefficients are averaged over 1000 realisations of the individual-level model.*

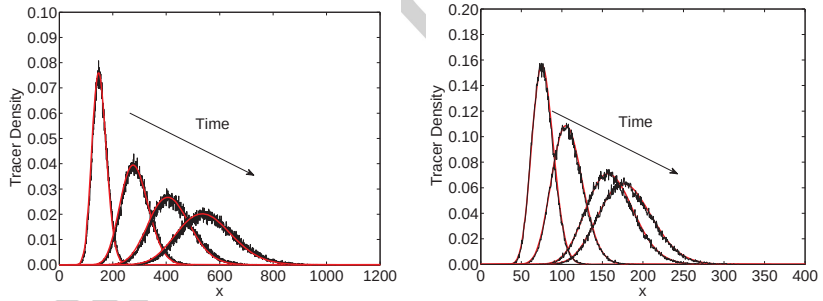

(a) (b)

Figure 11: *A comparison of the expected occupancy of tracer particles on domains growing according to (a) linear and (b) Gompertzian growth in the stochastic and deterministic regimes at different times. The coefficients of the FPE solved to find the red curves are determined using the coefficient estimation approach and are those displayed in Fig. 10. Figure descriptions and initial conditions are as in Fig. 3. Parameters are as in Fig. 10.* $\Delta = 1/2$ *in both cases.*

[3]Note that when employing the given coefficients in order to solve the associated FPE, we average the values of the drift and diffusion coefficient at each time-point over a window of size 10 (a convolution) in order to make the curves smoother.

ACCEPTED MANUSCRIPT

6. Discussion

Beginning with individual-based, stochastic models for the density of tracer particles on a discrete growing domain we have derived analytically the drift and diffusion coefficients of a set of PDEs which correspond to the expected tracer density. We have exemplified this stochastic-deterministic equivalence framework for a range of different time-dependent growth models. In each case we have attempted to provide a biological context in which such a growth process might occur. We note, however, that processes we have investigated are by no means exhaustive in terms of describing biological growth [30, 13]. Our generalised method allows the analytical derivation of the associated drift and diffusion coefficients for any time-dependent growth rate in the individual-based model. In addition, we have incorporated the possibility of elemental death into the individual-based model and derived the coefficients of the corresponding PDE for these general time-dependent birth and death rates. This approach highlights that a process in which both elemental birth and death occur cannot simply be approximated by a birth-only process with the reduced net growth rate since, although the drift coefficient may be correct, the diffusion coefficient will not be. Clearly, in situations in which the net birth rate is negative a simple birth process will not suffice.

For representative examples of our pure-birth, birth-death and pure-death processes we have carried out numerical simulations which contrast the expected tracer density in the individual-level model with the solution of the continuous PDE model. We see good agreement in each case with the correspondence increasing with decreasing element size, Δ. We suggest that FPE underestimates the density of tracer particles at the right-hand end of the domain where the infinitesimal moments, neglected by the FPE description of the individual-level process, are largest. The agreement between the two descriptions improves with decreasing Δ as the higher order moments become negligible.

We have also presented a Fokker-Plank coefficient estimation approach to deal with situations in which the infinitesimal moments cannot be derived analytically. Using short bursts of appropriately initialised stochastic simulation it is possible to approximate numerically the dependence of the drift and diffusion coefficients of an assumed underlying FPE on space and time. These coefficients

Accepted manuscript

ACCEPTED MANUSCRIPT

can then be used to solve the corresponding PDE for the tracer density. We verified our computer assisted approach in cases where the coefficients are known analytically and we were able to demonstrate that the solution of the PDE, with the approximated coefficients, gave a good representation of the expected density of the tracer particles.

As yet we have considered only the relatively straight-forward case of uniformly growing domains in which each element is selected to proliferate or die with equal probability. It is not immediately evident what effect, allowing anisotropic element proliferation will have on the corresponding drift and diffusion coefficients [11]. We have postulated that, even in situations where such coefficients can not be derived analytically, our coefficient estimation approach will still allow us to derive numerical approximations to such coefficients. A further challenge will lie in the adaptation of these methods to multivariate diffusion processes which will correspond to higher dimensional PDEs.

Since tissue growth is an important factor in the transport of cells across the domain, and often does not occur uniaxially or uniformly, these extensions will constitute an important step forward in our ability to model cell migration effectively at both and individual and collective level.

Appendix - Numerical solution of the PDE

In order to solve the PDE (4) we use we use a Lagrangian formulation, making a transformation of coordinates of the form [1, 9, 11, 8]

$$x = \Gamma(X, \tau) \quad \text{and} \quad Ct = \tau. \tag{60}$$

The advection due to domain growth is defined by the strain rate, $s = \mu_x$ satisfying

$$s = \frac{\Gamma_{X\tau}}{\Gamma_X}, \tag{61}$$

and the subscripts denote partial derivatives with respect to the appropriate variables. This leads to the system of PDEs:

$$C_\tau = \frac{1}{\Gamma_X}\left(\frac{\sigma^2 C_X}{2\Gamma_X}\right)_X - sC, \tag{62}$$

$$\Gamma_{X\tau} = s\Gamma_X, \tag{63}$$

Accepted manuscript

ACCEPTED MANUSCRIPT

where $\Gamma(X,0) = X$, $\Gamma(0,t) = 0$. The boundary conditions $C(0,t) = 0$ and $C(L(t)) = 0$ (where $L(t)$ is the deterministic domain length) are appropriate for tracer density which vanishes at the boundary.

We transform the system to one of first order and employ the NAG library routine D03PE and the MATLAB's NAG toolbox in order to solve the the PDEs numerically.

Acknowledgement

I would like to thank Christ Church, Oxford for the award of a Junior Research Fellowship. I would also like to thank Chris Lester for his helpful discussions.

7. References

[1] R.E. Baker and P.K. Maini. A mechanism for morphogen-controlled domain growth. *J. Math. Biol.*, 54(5):597–622, 2007.

[2] R.E. Baker, C.A. Yates, and R. Erban. From microscopic to macroscopic descriptions of cell migration on growing domains. *Bull. Math. Biol.*, 72 (3):719–762, 2010.

[3] B.J. Binder and K.A. Landman. Exclusion processes on a growing domain. *J. Theor. Biol.*, 259(3):541–551, 2009.

[4] B.J. Binder, K.A. Landman, M.J. Simpson, M. Mariani, and D.F. Newgreen. Modeling proliferative tissue growth: a general approach and an avian case study. *Phys. Rev. E*, 78(3):031912, 2008.

[5] A. Chevallier, M. Kieny, and A. Mauger. Limb-somite relationship: origin of the limb musculature. *Development*, 41(1):245–258, 1977.

[6] C.A. Chimenti, A.J. Hall, and M. Sol L'opez. Embryo-growth rate and duration in sunflower as affected by temperature. *Field. Crop. Res.*, 69(1): 81–88, 2001.

[7] E.J. Crampin and P.K. Maini. Modelling biological pattern formation: the role of domain growth. *Comments on Theoret. Biol*, 6:229–249, 2001.

Accepted manuscript

ACCEPTED MANUSCRIPT

[8] E.J. Crampin and P.K. Maini. Reaction-diffusion models for biological pattern formation. *Methods Appl. Anal.*, 8(2):415–428, 2001.

[9] E.J. Crampin, E.A. Gaffney, and P.K. Maini. Reaction and diffusion on growing domains: scenarios for robust pattern formation. *Bull. Math. Biol.*, 61(6):1093–1120, 1999.

[10] E.J. Crampin, E.A. Gaffney, and P.K. Maini. Mode-doubling and tripling in reaction-diffusion patterns on growing domains: A piecewise linear model. *J. Math. Biol.*, 44(2):107–128, 2002.

[11] E.J. Crampin, W.W. Hackborn, and P.K. Maini. Pattern formation in reaction-diffusion models with nonuniform domain growth. *Bull. Math. Biol.*, 64(4):747–769, 2002.

[12] D.C. Deeming and M.W.J. Ferguson. Morphometric analysis of embryonic development in *Alligator mississippiensis*, *Crocodylus johnstoni* and *Crocodylus porosus*. *J. Zool.*, 221(3):419–439, 1990.

[13] P. Gerlee. The model muddle: in search of tumor growth laws. *Cancer Res.*, 73(8):2407–2411, 2013.

[14] D.T. Gillespie. *Markov Processes: An Introduction for Physical Scientist*. Academic Press, 1992.

[15] B. Gompertz. On the nature of the function expressive of the law of human mortality, and on a new mode of determining the value of life contingencies. *Phil. Trans. R. Soc. A*, 115:513–583, 1825.

[16] D.G. Greenhalgh. The role of apoptosis in wound healing. *Int. J. Biochem. Cell. Biol.*, 30(9):1019–1030, 1998.

[17] F. Grinnell, M. Zhu, M.A. Carlson, and J.M. Abrams. Release of mechanical tension triggers apoptosis of human fibroblasts in a model of regressing granulation tissue. *Exp. Cell. Res.*, 248(2):608–619, 1999.

[18] J.D. Hywood, E.J. Hackett-Jones, and K.A. Landman. Modelling biological tissue growth: discrete to continuum representations. *Phys. Rev. E*, 88(3): 032704, 2013.

Accepted manuscript

ACCEPTED MANUSCRIPT

[19] S. Karlin and H.M. Taylor. *A second course in stochastic processes*, volume 2. Academic press, 1981.

[20] I.G. Kevrekidis, C.W. Gear, J.M. Hyman, P.G. Kevrekidis, O. Runborg, and C. Theodoropoulos. Equation-free, coarse-grained multiscale computation: enabling microscopic simulators to perform system-level analysis. *Comm. Math. Sci.*, 1(4):715–762, 2003.

[21] B. Korsgaard and F.Ø. Andersen. Embryonic nutrition, growth and energetics in *Zoarces viviparus L.* as indication of a maternal-fetal trophic relationship. *J. Comp. Physiol. B*, 155(4):437–444, 1985.

[22] P.M. Kulesa, G.C. Cruywagen, S.R. Lubkin, P.K. Maini, J.S. Sneyd, M.W.J. Ferguson, and J.D. Murray. On a model mechanism for the spatial patterning of teeth primordia in the alligator. *J. Theor. Biol.*, 180(4): 287–296, 1996.

[23] A. K. Laird. Dynamics of tumour growth. *Brit. J. Cancer*, 18(3):490, 1964.

[24] A.K. Laird. *Dynamics of normal growth*, volume 6971, page 52. Argonne National Laboratory, 1964.

[25] A.K. Laird. Dynamics of relative growth. *Growth*, 29(3):249, 1965.

[26] K.A. Landman, G.J. Pettet, and D.F. Newgreen. Mathematical models of cell colonization of uniformly growing domains. *Bull. Math. Biol.*, 65(2): 235, 2003.

[27] A. Leshem, A. Ar, and R.A. Ackerman. Growth, water, and energy metabolism of the soft-shelled turtle (*Trionyx triunguis*) embryo: effects of temperature. *Physiol. Zool.*, 64(2):568–594, 1991.

[28] R. McLennan, L. Dyson, K.W. Prather, J.A. Morrison, R.E. Baker, P.K. Maini, and P.M. Kulesa. Multiscale mechanisms of cell migration during development: theory and experiment. *Development*, 139(16):2935–2944, 2012.

[29] J.D. Murray, D.C. Deeming, and M.W.J. Ferguson. Size-dependent pigmentation-pattern formation in embryos of alligator mississippiensis:

Accepted manuscript

ACCEPTED MANUSCRIPT

time of initiation of pattern generation mechanism. *P. Roy. Soc. B-Biol. Sci.*, 239(1296):279–293, 1990.

[30] K.J. Painter, P.K. Maini, and H.G. Othmer. Stripe formation in juvenile *Pomacanthus* explained by a generalized Turing mechanism with chemotaxis. *Proc. Natl. Acad. Sci. USA.*, 96(10):5549–5554, 1999.

[31] T.N. Pettit, G.S. Grant, G.C. Whittow, H. Rahn, and C.V. Paganelli. Embryonic oxygen consumption and growth of Laysan and black-footed albatross. *Am. J. Physiol.-Reg. I.*, 242(1):121–128, 1982.

[32] M.J. Simpson, K.A. Landman, and D.F. Newgreen. Chemotactic and diffusive migration on a nonuniformly growing domain: numerical algorithm development and applications. *J. Comput. Appl. Math.*, 192(2):282–300, 2006.

[33] B. Westergaard and M.W.J. Ferguson. Development of the dentition in *Alligator mississippiensis*: Early embryonic development in the lower jaw. *J. Zool.*, 210(4):575–597, 1986.

[34] B. Westergaard and M.W.J. Ferguson. Development of the dentition in *Alligator mississippiensis*: Later development in the lower jaws of embryos, hatchlings and young juveniles. *J. Zool.*, 212(2):191–222, 1987.

[35] B. Westergaard and M.W.J. Ferguson. Development of the dentition in *Alligator mississippiensis*: Upper jaw dental and craniofacial development in embryos, hatchlings, and young juveniles, with a comparison to lower jaw development. *Am. J. Anat.*, 187(4):393–421, 1990.

[36] G.B. Whitham. *Linear and nonlinear waves*, volume 42. John Wiley & Sons, 2011.

[37] L. Wolpert. Positional information and the spatial pattern of cellular differentiation. *J. Theor. Biol.*, 25(1):1–47, 1969.

[38] T.E. Woolley, R.E. Baker, E.A. Gaffney, and P.K. Maini. Stochastic reaction and diffusion on growing domains: Understanding the breakdown of robust pattern formation. *Phys. Rev. E*, 84(4):046216, 2011.

Accepted manuscript

ACCEPTED MANUSCRIPT

[39] C.A. Yates, R. Erban, C. Escudero, I.D. Couzin, J. Buhl, I.G. Kevrekidis, P.K. Maini, and D.J.T. Sumpter. Inherent noise can facilitate coherence in collective swarm motion. *Proc. Natl. Acad. Sci. USA.*, 106(14):5464–5469, 2009.

[40] C.A. Yates, R.E. Baker, R. Erban, and P.K. Maini. Going from microscopic to macroscopic on non-uniform growing domains. *Phys. Rev. E*, 86(2): 021921, 2012.

Accepted manuscript